1521-0103/12/3432-479–488$25.00
THE JOURNAL OF PHARMACOLOGY AND EXPERIMENTAL THERAPEUTICS
JPET 343:479–488, 2012

Vol. 343, No. 2
195446/3802941

Vinpocetine Suppresses Pathological Vascular Remodeling by Inhibiting Vascular Smooth Muscle Cell Proliferation and Migration[S]

Yujun Cai, Walter E. Knight, Shujie Guo, Jian-Dong Li, Peter A. Knight, and Chen Yan

Aab Cardiovascular Research Institute and Department of Medicine (Y.C., W.E.K., C.Y.) and Department of Surgery (P.A.K.), University of Rochester, Rochester, New York; Shanghai Key Laboratory of Vascular Biology at Ruijing Hospital, Shanghai Jiaotong University School of Medicine, Shanghai, China (S.G., C.Y.); and Center for Inflammation, Immunity, and Infection and Department of Biology, Georgia State University, Atlanta, Georgia (J.-D.L.)

Received April 13, 2012; accepted August 16, 2012

ABSTRACT

Abnormal vascular smooth muscle cell (SMC) activation is associated with various vascular disorders such as atherosclerosis, in-stent restenosis, vein graft disease, and transplantation-associated vasculopathy. Vinpocetine, a derivative of the alkaloid vincamine, has long been used as a cerebral blood flow enhancer for treating cognitive impairment. However, its role in pathological vascular remodeling remains unexplored. Herein, we show that systemic administration of vinpocetine significantly reduced neointimal formation in carotid arteries after ligation injury. Vinpocetine also markedly decreased spontaneous remodeling of human saphenous vein explants in ex vivo culture. In cultured SMCs, vinpocetine dose-dependently suppressed cell proliferation and caused G_1-phase cell cycle arrest, which is associated with a decrease in cyclin D1 and an increase in $p27^{Kip1}$ levels. In addition, vinpocetine dose-dependently inhibited platelet-derived growth factor (PDGF)-stimulated SMC migration as determined by the two-dimensional migration assays and three-dimensional aortic medial explant invasive assay. Moreover, vinpocetine significantly reduced PDGF-induced type I collagen and fibronectin expression. It is noteworthy that PDGF-stimulated phosphorylation of extracellular signal-regulated kinases 1/2 (ERK1/2), but not protein kinase B, was specifically inhibited by vinpocetine. Vinpocetine powerfully attenuated intracellular reactive oxidative species (ROS) production, which largely mediates the inhibitory effects of vinpocetine on ERK1/2 activation and SMC growth. Taken together, our results reveal a novel function of vinpocetine in attenuating neointimal hyperplasia and pathological vascular remodeling, at least partially through suppressing ROS production and ERK1/2 activation in SMCs. Given the safety profile of vinpocetine, this study provides insight into the therapeutic potential of vinpocetine in proliferative vascular disorders.

Introduction

One of the important pathological hallmarks in pathological vascular remodeling is the abnormal accumulation of smooth muscle-like cells that are characterized primarily by expressing SMC marker α-smooth muscle actin and morphologically and functionally resemble myofibroblasts. These cells are frequently referred to as "synthetic SMCs," because it has long been believed that these cells are derived from the phenotypic modulation of medial SMCs from a contractile phenotype to a synthetic one (Owens et al., 2004; Doran et al., 2008). New evidence also supports the possible transdifferentiation of adventitial fibroblasts (Sartore et al., 2001) or the differentiation of progenitor cells to these SMC-like cells (Sata et al., 2002; Torsney and Xu, 2011). Regardless of origins, synthetic SMCs are evidently proproliferative, promigratory, proinflammatory, and promatrix remodeling, playing key roles in the development of various vascular disorders such as atherosclerosis, postangioplasty restenosis,

This research was supported by the National Institutes of Health National Heart, Lung, and Blood Institute [Grants HL077789; HL088400] (to C.Y.); the American Heart Association [Grant 0740021N] (to C.Y.); and a Shanghai Oriental Scholarship (to C.Y.).
Article, publication date, and citation information can be found at http://jpet.aspetjournals.org.
http://dx.doi.org/10.1124/jpet.112.195446.
[S] The online version of this article (available at http://jpet.aspetjournals.org) contains supplemental material.

ABBREVIATIONS: SMC, smooth muscle cell; VSMC, vascular SMC; 3D, three-dimensional; AKT, protein kinase B; p-AKT, phosphorylated AKT; BrdU, bromodeoxyuridine; DAPI, 4,6-diamidino-2-phenylindole; $DCFH_2$-DA, dichlorodihydrofluorecein diacetate; DMEM, Dulbecco's modified Eagle's medium; ECM, extracellular matrix; ERK1/2, extracellular signal-regulated kinase 1/2; p-ERK, phosphorylated ERK; FBS, fetal bovine serum; FGF, fibroblast growth factor; IKK, IκB kinase; LCA, left carotid artery; NAC, *N*-acetyl-L-cysteine; PBS, phosphate-buffered saline; PCNA, proliferating cell nuclear antigen; PCR, polymerase chain reaction; PDE1, phosphodiesterase 1; PDGF, platelet-derived growth factor; ROS, reactive oxygen species; SRB, sulforhodamine-B; SV, saphenous vein; Vinp, vinpocetine.

bypass vein graft failure, and allograft vasculopathy (Ross, 1993; Kearney et al., 1997; Mitchell and Libby, 2007). Thus, inhibiting SMC proliferation represents a therapeutic strategy to antagonize proliferative vascular remodeling. For example, for preventing restenosis after percutaneous coronary intervention the most effective therapy is local delivery of antiproliferative reagents via drug-eluting stents containing sirolimus (Moses et al., 2003) or paclitaxel (Stone et al., 2004). Sirolimus and paclitaxel inhibit SMC proliferation by targeting mammalian target of rapamycin and microtubule formation, respectively. However, there are some major concerns regarding the endothelial toxicity of these stents, which may attenuate re-endothelization, leading to increased stent thrombosis, particularly after patients stop taking antiplatelet therapy (Pendyala et al., 2009). In addition, drug-eluting stenting has limited impact on other vascular disorders with diffuse neointimal lesions. Therefore, developing novel and systemically safe agents is currently in high demand.

Vinpocetine is produced by slightly altering the vincamine molecule, an alkaloid extracted from the periwinkle plant, *Vinca minor* (Bönöczk et al., 2000). Vinpocetine was originally discovered and marketed in 1978 under the trade name Cavinton (Gedeon Richter, Budapest, Hungary). Since then, vinpocetine has been widely used in many countries for the preventive treatment of cognitive impairment, including stroke, senile dementia, and memory disturbances (Bagoly et al., 2007). For instance, different types of vinpocetine-containing memory enhancers [such as Intelectol (Memory Secret, Miami, FL) and Memolead (Kao Kabushiki Kaisha, Tokyo, Japan)] are currently used as dietary supplements. To date, there have been no reports of significant side effects, toxicity, or contraindications at therapeutic doses of vinpocetine. Mechanistically, vinpocetine acts as a cerebral vasodilator that improves brain blood flow (Tamaki and Matsumoto, 1985). Vinpocetine has also been shown to act as a cerebral metabolic enhancer by increasing oxygen and glucose uptake from blood and stimulating neuronal ATP production (Szobor and Klein, 1976). Vinpocetine seems to affect several cellular targets, such as Ca^{2+}/calmodulin-stimulated cyclic nucleotide phosphodiesterase 1 (PDE1) and voltage-dependent Na^{+} channels (Bönöczk et al., 2000). We have found that IκB kinase (IKK) is a new cellular target of vinpocetine, and vinpocetine attenuates tumor necrosis factor-α-induced nuclear factor κB activation and the subsequent induction of proinflammatory mediators in multiple cell types, including vascular smooth muscle cells, endothelial cells, and macrophages (Jeon et al., 2010b). In vasculature, vinpocetine has been shown previously to cause vascular relaxation (Kim et al., 2001). In this study, we explore the role and underlying mechanism of vinpocetine in SMC proliferation, migration, extracellular matrix (ECM) production, and pathological vascular remodeling.

Materials and Methods

Animals. All animals were used in accordance with the guidelines of the National Institutes of Health (Institute of Laboratory Animal Resources, 1996) and American Heart Association for the care and use of laboratory animals. The procedures were performed in accordance with experimental protocols that were approved by the University Committee on Animal Resources at the University of Rochester. FVB/NJ mice were purchased from The Jackson Laboratory (Bar Harbor, ME). Animals were housed under a 12-h light-dark regimen.

Common Carotid Artery Ligation. Eight-week-old male FVB/NJ mice were used in all animal experiments. Complete common carotid artery ligation was performed as described previously (Kumar and Lindner, 1997). Mice were anesthetized with inhaled isoflurane. The left common carotid artery was dissected through a small midline incision in the neck and completely ligated with 6-0 silk sutures just proximal to the common carotid bifurcation. In the sham group, the suture was passed under the exposed carotid artery but not ligated. For systemic vinpocetine treatment, mice were intraperitoneally injected with 5 mg/kg vinpocetine every day as described previously (Jeon et al., 2010b). Mice were sacrificed 14 days after carotid ligation. In brief, mice were anesthetized by intraperitoneal injection with 80 $mg \cdot kg^{-1}$ ketamine and 5 $mg \cdot kg^{-1}$ xylazine, perfused with saline, and fixed in 10% phosphate-buffered formaldehyde. Carotid arteries were dissected and embedded in paraffin. Sections were cut at 200-μm intervals. The cumulative results of luminal, intimal, and medial areas from eight animals were obtained. Morphometric analysis was performed on an average of 10 sequential sections at 200 μm apart and downstream of the ligation site of the left carotid artery (LCA).

Immunohistochemistry. Vessels were embedded in paraffin, and cross-sections were cut at 200-μm intervals. The sections were deparaffinized, followed by treatment with citrate buffer for antigen retrieval and 3% H_2O_2. The sections were blocked with Dako serum-free blocking solution (Dako North America, Inc., Carpinteria, CA) and incubated with primary antibody overnight at 4°C. The primary antibodies included α-smooth muscle actin (Dako North America, Inc.) and PCNA (BD Biosciences, San Jose, CA). Subsequently, the sections were incubated with biotinylated secondary antibodies for 30 min at room temperature. Avidin-biotinylated enzyme complex (Vector Laboratories, Burlingame, CA) and a diaminobenzidine substrate chromogen system (Dako North America, Inc.) were used for detection. Sections were counterstained with hematoxylin. As a negative control, matched IgG was used in place of the primary antibody. Slides were viewed with a microscope (BX41; Olympus, Tokyo, Japan) and a digital camera (Spot Insight 2; Diagnostic Instruments, Inc., Sterling Heights, MI).

Ex Vivo Culture of Human Saphenous Veins. Human saphenous veins (SVs) were collected from patients after coronary artery bypass surgery and performed as described previously (Ranjzad et al., 2009). In brief, the SVs were opened longitudinally and cut transversely into 0.5-cm segments. These segments were pinned onto Mersilene mesh (Ethicon, Cornelia, GA) with luminal surface facing up and cultured individually in 12-well plates in RPMI 1640 medium supplemented with 30% fetal bovine serum (FBS), 2 mM L-glutamine, 100 IU/ml penicillin, and 100 μg/ml streptomycin for 7 days at 37°C with 5% CO_2. Culture media and drug were replaced every other day. At the end of the culturing, the vein segments were washed in phosphate-buffered saline (PBS), fixed with 10% phosphate-buffered formalin for 24 h, and embedded in paraffin, and cross-sections (5 μm) were prepared.

BrdU Immunofluorescent Staining. Proliferation of cells from ex vivo cultured SV was assessed by BrdU incorporation (Porter et al., 1996). In brief, SV segments were cultured for 4 days and then treated with 10 μM BrdU, which was allowed to incorporate for 3 days. SV were fixed with formalin and embedded in paraffin, and cross-sections were cut. The sections were deparaffinized, followed by treatment with citrate buffer for antigen retrieval and blocked with Dako serum-free blocking solution (Dako North America, Inc.) and incubated with anti-BrdU fluorescein antibody (Roche Diagnostics, Indianapolis, IN). For α-smooth muscle actin staining, Cy3-conjugated α-smooth muscle actin antibody (Sigma, St. Louis, MO) were used. Nuclei were stained with DAPI. Images were captured with an Olympus (BX-51) fluorescent microscope.

3D Ex Vivo Aortic Medial Explant Migration Assay. 3D collagen matrices (final concentration 2.7 mg/ml) were prepared by neutralizing the collagen-I solution with 1/6 volume of 6× Dulbecco's modified Eagle's medium (DMEM) and diluting it to a final volume with 1× DMEM (Filippov et al., 2005). In brief, each mouse thoracic

aorta was dissected, the adventitia was stripped by collagenase type II digestion, and the endothelium layer was removed. The media explants were then cut into 1-mm fragments, suspended within type I collagen solution, and cultured for 8 days in DMEM supplemented with 10% FBS. A mixture of PDGF-BB/FGF-2 (10 ng/ml each; R&D Systems, Minneapolis, MN) was added to explant cultures to initiate SMC outgrowth and migration. Cell migration was quantified by measuring the distance migrated by the leading front of SMCs from the explanted tissue.

Rat Aortic Smooth Muscle Cell Culture. Rat aortic SMCs were prepared by using enzymatic digestion of aortas from 10-week-old Sprague-Dawley rats (The Jackson Laboratory) as described previously (Nagel et al., 2006). SMCs were grown in DMEM containing 10% FBS in a humidified incubator (37°C, 5% CO_2). SMCs (passages 7–12) were used for the experiments.

Cell Growth. Cell growth was evaluated by measuring cellular protein content using the sulforhodamine-B (SRB) colorimetric assay (Vichai and Kirtikara, 2006). SMCs were seeded in 96-well plates overnight in DMEM supplemented with 10% FBS, serum-starved for 2 days, treated with vehicle or vinpocetine, and stimulated by 5% FBS or 50 ng/ml PDGF-BB for the indicated times. Cells were fixed, washed, dried, stained, and solubilized. Optical density was measured at 515 nm by using a microplate spectrophotometer (VersaMax; Molecular Devices, Sunnyvale, CA).

Cell Cycle Assessment. The distribution of SMCs at different stages in the cell cycle was estimated by flow cytometric DNA analysis. In brief, cells were seeded overnight in DMEM containing 10% FBS, serum-starved for 2 days, then treated with or without vinpocetine and stimulated with 5% FBS for 24 h. Cells were harvested and washed with PBS, pH 7.4, and then fixed with 70% ethanol in PBS at 4°C. After PBS washing, the pellet was dissolved in RNaseA solution (20 μg/ml) and incubated at 37°C for 15 min, and then stained with propidium iodide for 30 min in the dark at room temperature. For each sample, at least 1×10^4 cells were analyzed using a FACS-Calibur cytometer (BD Biosciences), and the percentage of cells in each cell cycle phase was calculated by using CellQuest software (BD Biosciences).

Scratch Wound Assays. SMCs were seeded in 35-mm dishes in DMEM overnight. Confluent cells were starved and scratched with a 100-μl pipette tip (Liang et al., 2007). The cells were pretreated with vehicle or vinpocetine and then stimulated with 25 ng/ml of PDGF-BB for 16 h. The cells were fixed with 4% paraformaldehyde and stained with hematoxylin. Images were captured by microscopes (BX41; Olympus) and a digital camera (Spot Insight 2; Diagnostic Instruments, Inc.). Quantification was made by using Image-Pro 6.2 software (Media Cybernetics, Inc., Bethesda, MD).

Boyden Chamber Assays. SMCs were trypsinized and resuspended at a concentration of 5×10^5 cells/ml in DMEM supplemented with 0.5% FBS. Microchemotaxis chambers and polycarbonate filters (Corning Glassworks, Corning, NY) were used. SMC suspension (100 μl) was placed in the upper chamber, and 600 μl of DMEM containing 25 ng/ml of PDGF-BB was placed in the lower chamber. The chamber was incubated at 37°C and 5% CO_2 for 6 h. The filter was then removed, and the cells on the upper side of the filter were scraped off with a cotton tip. The filter membrane were fixed in 4% paraformaldehyde and stained with hematoxylin. The images were viewed and captured by microscopes (BX41; Olympus) and a digital camera (Spot Insight 2; Diagnostic Instruments, Inc.).

F-Actin Cytoskeleton Staining. SMCs were seeded on 35-mm glass-bottom dishes in DMEM supplemented with 10% FBS overnight, serum-starved for 2 days, pretreated with vehicle or vinpocetine, and stimulated by 20 ng/ml PDGF-BB for 24 h. Cells were fixed with 4% paraformaldehyde for 10 min and permeabilized in 0.2% Triton X-100 for 5 min at room temperature. Cells were incubated with Alexa Fluor 546 phalloidin (Invitrogen, Carlsbad, CA) for 1 h at room temperature. The nuclear was stained with DAPI. Images of F-actin were captured with an Olympus (BX-51) fluorescent microscope.

ROS Analysis. Accumulation of intracellular ROS was detected with the probe $DCFH_2$-DA as described previously (Cai et al., 2008). In brief, after treatment, cells were labeled with 10 μM $DCFH_2$-DA for 20 min at 37°C in a humidified atmosphere at 5% CO_2. The labeled cells were washed and immediately photographed by using an Olympus (BX-51) fluorescent microscope. To quantify ROS, the fluorescence intensity was measured by flow cytometry (FACSCalibur, BD Biosciences).

[^{3}H]Proline Incorporation. Collagen synthesis was determined by assessing [^{3}H]proline incorporation (Callera et al., 2005). SMCs were seeded in 12-well plates in DMEM supplemented with 10% FBS overnight, then starved for 2 days. The cells were treated with vinpocetine and stimulated by 20 ng/ml PDGF-BB for 18 h, then pulsed for an additional 6 h by the addition of 1 μCi/ml [^{3}H]proline. Cells were then washed twice with cold PBS and incubated in 10% trichloroacetic acid for 30 min on ice to precipitate protein. Precipitates were washed twice with cold 95% ethanol, solubilized in 0.5 N NaOH for 30 min, and neutralized with 1 N HCl. Radioactivity was quantified by using a liquid scintillation counter. Samples were normalized to total precipitable protein per well as measured by Bradford assay.

Western Blot Analysis. Western blot analysis was performed as described previously (Nagel et al., 2006). In brief, lysates were prepared in radioimmunoprecipitation assay buffer with protease inhibitor cocktail (Sigma). The cell lysates were loaded on SDS-polyacrylamide gel electrophoresis, electrophoresed, and transferred onto the polyvinylidene difluoride membranes. The membranes were blocked in 5% nonfat dry milk in 0.01% Tween/PBS, incubated in primary antibody overnight at 4°C, then incubated in horseradish peroxidase-conjugated secondary antibodies and developed by using Enhanced Chemiluminescence Plus detection reagent. The primary antibodies used in this study were: collagen-I (kindly provided by Dr. Larry W. Fisher, National Institutes of Health, Bethesda, MD), fibronectin (kindly provided by Dr. Jane Sottile, University of Rochester, Rochester, NY), p-ERK (Cell Signaling Technology, Danvers, MA), ERK (Cell Signaling Technology), p-AKT (Cell Signaling Technology), AKT (Cell Signaling Technology), and β-actin (Santa Cruz Biotechnology, Inc., Santa Cruz, CA). For measuring secreted collagen I and fibronectin, cell mediums were filtered and analyzed by Western blotting procedure.

RNA Isolation and Real-Time PCR. Total cellular RNA was isolated from SMCs by using an RNeasy Mini Kit (QIAGEN, Valencia, CA) according to the manufacturer's instructions. RNA was subjected to reverse transcription by using a Taqman reverse transcription kit (Applied Biosystems, Foster City, CA) following the manufacturer's instructions. Real-time PCR amplifications were performed by using iQTM SYBR Green supermix (Bio-Rad Laboratories, Hercules, CA). The relative quantities of mRNAs were obtained by using the comparative Ct method and normalized with glyceraldehyde-3-phosphate dehydrogenase. The primer sequences were as follows: rCyclin D1, forward primer 5′-GCTGCAAATGGAACTGCTTCTGGT-3′ and reverse primer 5′-AAGGTCTGTGCATGTTTGCGGATG-3′; rP21^{Cip1}, forward primer 5′-TGCCTGGTTCCTTGCCACTTCTTA-3′ and reverse primer 5′-AGGCTGTGACTGCTTCACTGTCAT-3′; rP27^{Kip1}, forward primer 5′-AGCTTGCCCGAGTTCTACTACAGA-3′ and reverse primer 5′-TTTGCCTGAGACCCAATTGAAGGC-3′; and glyceraldehyde-3-phosphate dehydrogenase, forward primer 5′-TCAAGAAGGTGGTGAAGCAG-3′ and reverse primer 5′-TGGGAGTTGCTGTTGAAGTC-3′.

Statistical Analysis. Quantitative results are expressed as mean ± S.D. All results shown were confirmed by at least three independent experiments. Data were analyzed by one-way analysis of variance. P values < 0.05 were considered statistically significant.

Results

Vinpocetine Reduced Neointima Formation after Carotid Ligation Injury in Mice. To determine whether

vinpocetine blocks pathological vascular remodeling, we performed complete LCA ligation surgery in mice, a procedure that is known to induce intimal hyperplasia caused by blood flow cessation (Kumar and Lindner, 1997). As shown in Fig. 1A, there is no obvious change in the appearance of LCA from sham-operated animals that received systemic intraperitoneal application of either vehicle or 5 mg/kg/day vinpocetine. Mice that underwent LCA ligation for 2 weeks developed significant neointima formation, but this remodeling was dramatically reduced by vinpocetine treatment. Morphometric analyses revealed that ligation injury caused a dramatic increase in intimal and medial thickening (Fig. 1B) and decrease in the lumenal area of the vessel (Fig. 1C) compared with sham operation. However, these changes were significantly diminished by vinpocetine treatment. In addition, the occurrence of thrombosis (Supplemental Fig. S1) and intraplaque hemorrhage (Fig. 1A) were prevented by vinpocetine. Because vascular smooth muscle cell proliferation is a crucial step for developing neointima hyperplasia, we conducted staining for PCNA (a cell proliferation marker) in carotid arteries (Fig. 1D). SMCs were counterstained with smooth muscle α-actin antibody. There was a significant increase in the number of PCNA-positive SMCs in ligated carotid arteries compared with sham arteries, whereas there was an approximately 50% reduction in the number of PCNA-positive cells in vinpocetine-treated mice (Fig. 1E).

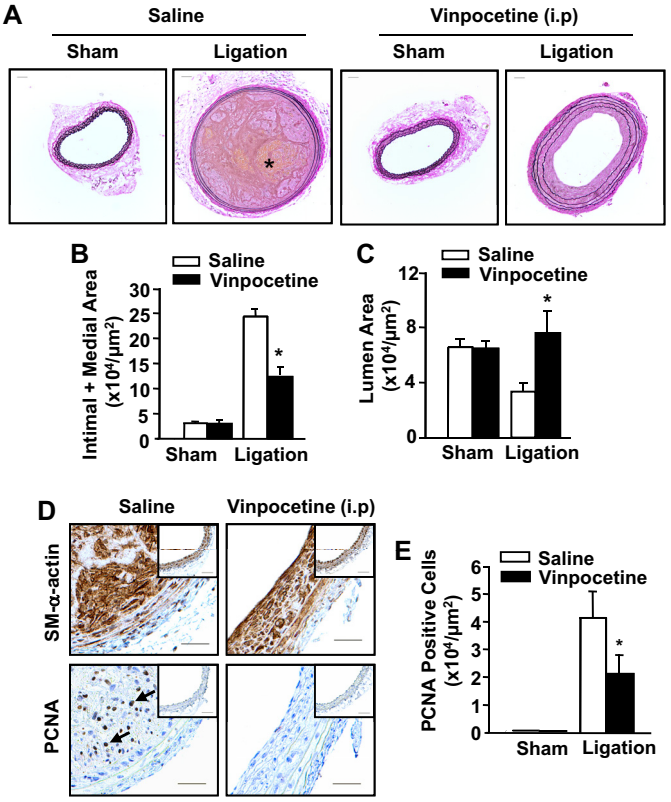

Fig. 1. Effects of systemic administration of vinpocetine on ligation injury-induced neointima formation. A, representative histological images of left common carotid arteries stained with Verhoeff-van Gieson from mice subjected to complete carotid ligation or sham operation for 14 days with systemic administration of vinpocetine (5 mg/kg/day) or vehicle saline intraperitoneally. Bar, 100 μm. Blue-black indicates elastic fibers. * indicates yellowish intraplaque hemorrhage. B and C, morphometric analyses show that vinpocetine decreases intimal + medial areas (B) and increases luminal areas (C) at 14 days after ligation. Values are means ± S.E.M. ($n = 8$ for saline and 10 for vinpocetine). *, $P < 0.05$ compared with saline under ligation. D, immunohistochemical analyses showing vinpocetine decreases cell proliferation as stained with PCNA. Insets are corresponding images of sham-operated samples. Brown staining represents smooth muscle SM-α-actin or PCNA. Blue represents counterstaining with hematoxylin. Bar, 100 μm. E, quantitative data of PCNA-positive cells. *, $P < 0.05$ compared with saline under ligation.

Vinpocetine Inhibits the Remodeling of Human Saphenous Vein in Ex Vivo. Human SV is the most commonly used vessel in coronary artery bypass grafts. Late vein graft failure occurs because of the development of stenosis or occlusion (Bhardwaj et al., 2008). When human SVs are cultured in vitro, they spontaneously undergo remodeling, which predominantly involves smooth muscle cell growth and ECM deposition (Mekontso-Dessap et al., 2006). This leads to an increased thickness of the SV vessel wall. The SV wall can be divided into three zones, the internal zone (intima), the medial zone (inner and outer media), and the external zone (inner and outer adventitia) (Cai et al., 2011). With Verhoeff Masson trichrome combination staining, smooth muscles are stained with red, collagen with light blue or blue-green, and elastin with dark blue (Fig. 2A). When SVs were cultured ex vivo for 7 days, SV wall thickness was profoundly increased in all three zones compared with the same vein without culture, and remodeling was significantly reduced by treatment with vinpocetine (Fig. 2, A and B). Consistently, the proliferating index measured by BrdU incorporation was also decreased by vinpocetine (Fig. 2, C and D).

Vinpocetine Inhibits SMC Proliferation. To understand the mechanism underlying vinpocetine-mediated attenuation of vascular remodeling, we isolated and cultured SMCs that are proliferatory and migratory and represent the cell type involved in intimal hyperplasia. As shown in Fig. 3A, cell proliferation was assessed by SRB assay, a well established colorimetric cell viability and proliferation assay (Vichai and Kirtikara, 2006). Serum-starved SMCs rapidly grew after stimulation with FBS in a time-dependent manner. However, these changes were attenuated in a dose-dependent manner by vinpocetine. In addition, we did not observe significant apoptosis or necrosis by vinpocetine treatment in these SMCs (data not shown).

Next, we evaluated the effects of vinpocetine on cell cycle progression by flow cytometric analysis. As shown in Fig. 3B, when SMCs underwent serum starvation approximately 95% of cells were synchronized in the G_1 phase of the cell cycle. The percentage of cells in S phase was increased after stimulation by FBS for 24 h. In contrast, vinpocetine significantly inhibited FBS-induced G_1/S transition in a dose-dependent manner. These data suggest that vinpocetine attenuates cell proliferation through inhibiting G_1/S transition.

To further delineate the mechanism of cell cycle arrest by vinpocetine, the effects of vinpocetine on G_1 arrest-relevant regulators were investigated. As shown in Fig. 3, C and D, the cyclin D1 was up-regulated, and the $p27^{Kip1}$ was down-regulated on both mRNA and protein levels. However, these changes were significantly inhibited by vinpocetine in a dose-dependent manner. These results suggest that vinpocetine arrests the G_1 phase by up-regulating $p27^{Kip1}$ and down-regulating cyclin D1 in SMCs.

Vinpocetine Inhibits Migration of SMCs. SMC migration from media to intima occurs in response to vascular injury (Schwartz and Henry, 2002). PDGF is a key factor in vascular injury-induced migration of SMCs (Raines, 2004). To examine the potential effect of vinpocetine on the migra-

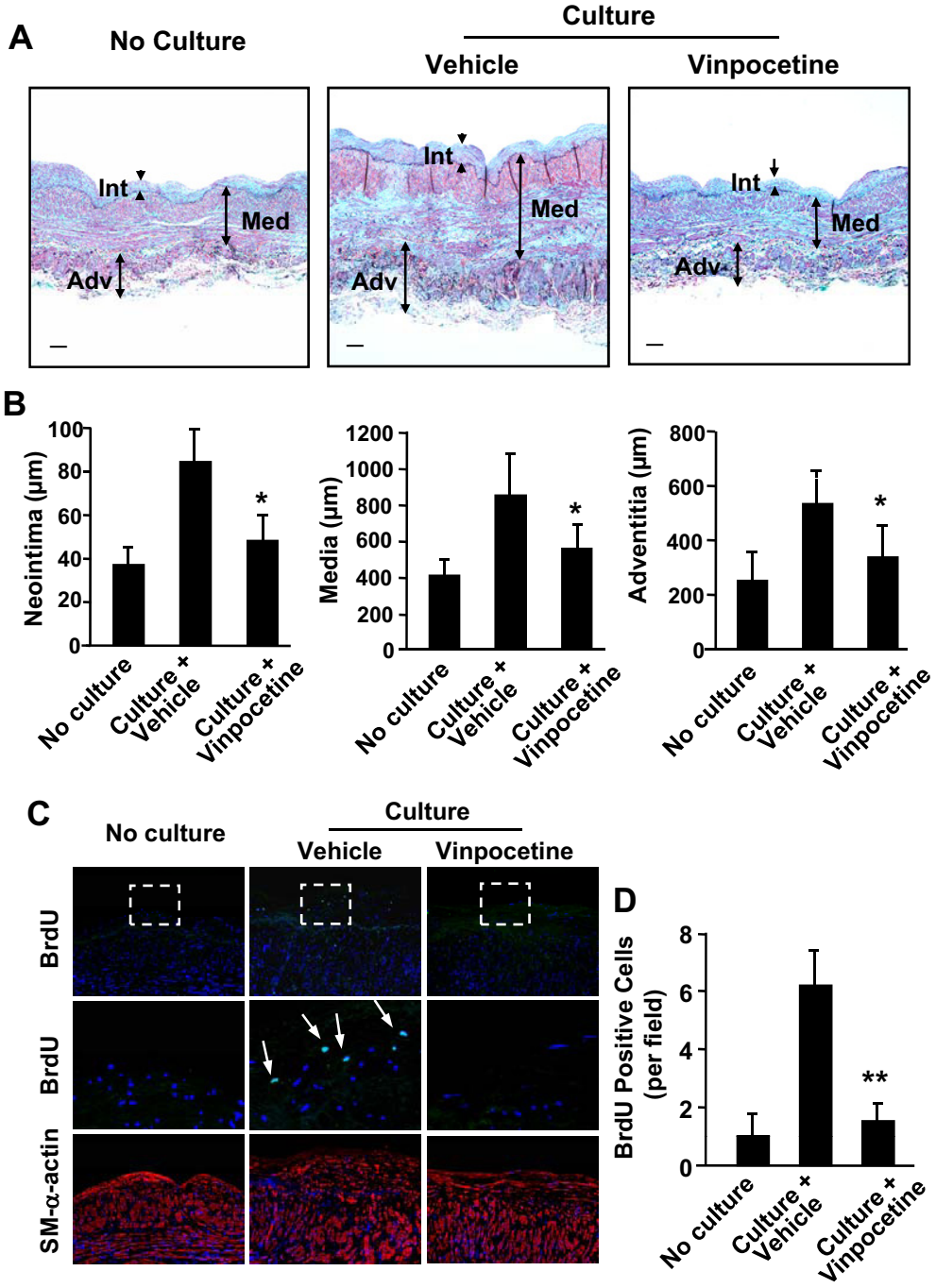

Fig. 2. Effects of vinpocetine on human saphenous vein remodeling in ex vivo organ culture. A, representative images of sections with Verhoeff Masson trichrome combination staining. Sections are from human saphenous vein before or after culture for 7 days in the presence of vehicle or 100 μM vinpocetine. Smooth muscles are stained with red, collagen with light blue or blue-green, and elastin with dark blue. Bar, 50 μm. Int, intima; Med, media; Adv, adventitia. B, quantification of thickness of intima, media, and adventitia. Values are means ± S.E.M. ($n = 6$). C, immunofluorescent images of human saphenous vein sections immunostained with BrdU or smooth muscle-α-actin. Middle panels are magnified images corresponding to the dotted-line squares in upper panels. The proliferative cells were stained with BrdU. Arrows point to BrdU-positive cells. D, quantification of BrdU-positive cells. **, $P < 0.01$ compared with control.

tion of SMCs, we first performed a scratch wound assay, a two-dimensional migration model (Goncharova et al., 2006). As shown in Fig. 4, A to C, PDGF-BB stimulation for 16 h induced profound migration. In contrast, vinpocetine dose-dependently decreased PDGF-BB-induced migration when quantified by both gap (Fig. 4B) and migration cells (Fig. 4C). To confirm the inhibitory effect of vinpocetine on migration, a modified Boyden chamber assay was also used to measure migration (Filippov et al., 2005). Consistently, vinpocetine dose-dependently inhibited PDGF-BB-induced migration of SMCs (Fig. 4, D and E). Moreover, we examined the effects of vinpocetine on 3D migration by using an ex vivo invasive assay in collagen matrix. As shown in Fig. 4, F and G, when mouse aortic media explants were treated with PDGF/FGF and cultured for 8 days in collagen I matrix SMCs migrated from media explant and infiltrated the collagen gel. In contrast, the outgrowth of SMCs from explant was significantly suppressed by vinpocetine.

Substantial evidence supports that actin cytoskeleton polymerization is critical during cell motility and migration (Gerthoffer, 2007). To further characterize the mechanisms by which vinpocetine inhibits migration in SMCs, actin filaments (F-actin) were stained with AlexaFluor 488-labeled phalloidin in SMCs. Figure 4H shows that actin polymerization was significantly increased in response to PDGF-BB stimulation. In contrast, this alteration was reversed by vinpocetine in a dose-dependent manner, suggesting that the regulation of actin cytoskeleton polymerization represents one of the mechanisms by which vinpocetine inhibits SMC migration.

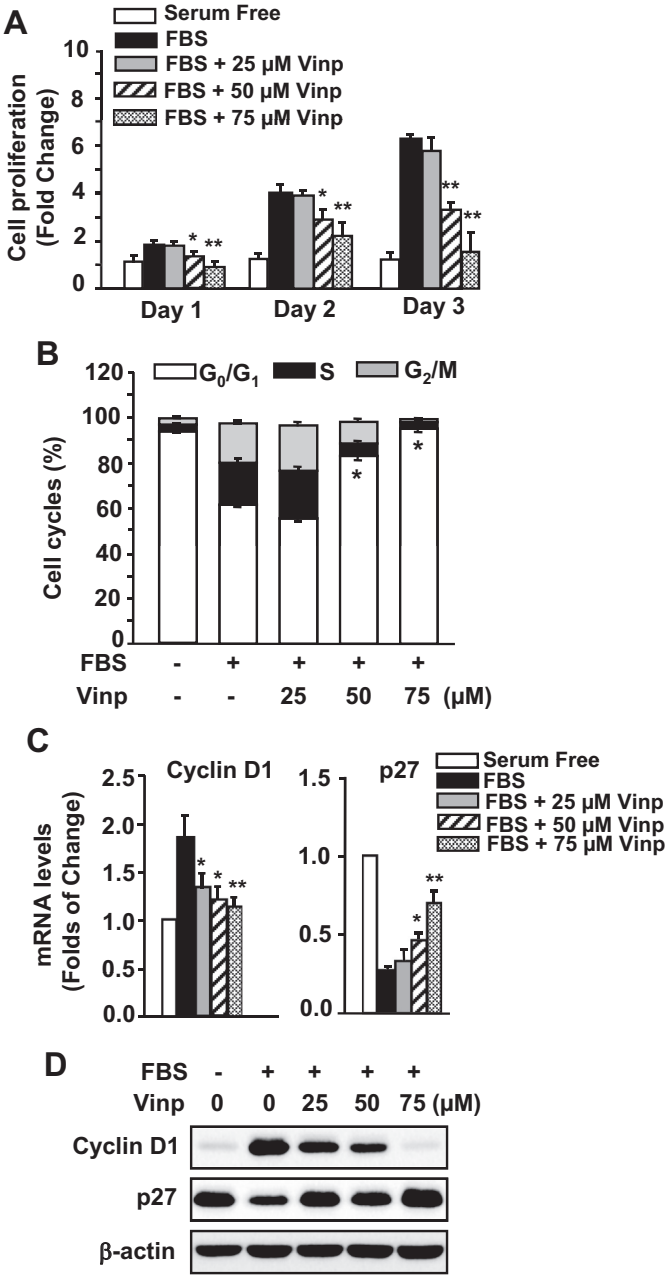

Fig. 3. Effects of vinpocetine (Vinp) on VSMC proliferation and cell cycle regulation. A, vinpocetine dose-dependently inhibited 5% FBS-induced proliferation of VSMCs. The cell proliferation was measured by SRB assay as described under *Materials and Methods*. B, vinpocetine promotes G_1 cell cycle arrest of VSMCs in a dose-dependent manner. Cell cycle was measured by flow cytometric DNA analysis as described under *Materials and Methods*. C, vinpocetine down-regulates cyclin D1 and up-regulates and $p27^{Kip1}$. VSMCs were serum-starved for 48 h and pretreated with vehicle or vinpocetine at the indicated doses, followed by stimulation with 5% FBS for 6 h. The expression of cyclin D1 and $p27^{Kip1}$ was analyzed by real-time PCR. Values are means ± S.D. from at least three independent experiments. *, $P < 0.05$; **, $P < 0.01$ versus FBS with zero vinpocetine. D, vinpocetine down-regulates cyclin D1 and up-regulates $p27^{Kip1}$ protein measured by Western blotting.

Vinpocetine Antagonizes PDGF-Induced ECM Synthesis in SMCs. ECM production plays a key role during atherogenesis and development of intimal hyperplasia. Fibronectin and collagen are the most common ECM proteins in pathological vascular remodeling (Adiguzel et al., 2009). To investigate the effect of vinpocetine on total collagen synthesis, we performed a [^{3}H]proline incorporation assay. As shown in Fig. 5A, the incorporation of [^{3}H]proline was dramatically increased when serum-starved SMCs were stimulated with PDGF-BB for 24 h. Vinpocetine significantly inhibited PDGF-BB-induced [^{3}H]proline incorporation in a dose-dependent manner. To further confirm the effect of vinpocetine on ECM expression, we measured intracellular and secreted type I collagen and fibronectin. As shown in Fig. 5, B and C, PDGF-BB markedly induced the expression of intracellular and secreted type I collagen and fibronectin. However, these effects were antagonized in the presence of vinpocetine.

Vinpocetine Blocks PDGF-Induced ERK1/2 Activation in SMCs. It is known that PDGF-BB stimulates the activation of several signaling pathways such as the ERK1/2 and phosphatidylinositol 3-kinase/AKT pathways, which are important in SMC growth and migration (Andrae et al., 2008). To further study the mechanisms of vinpocetine's antagonistic effects on SMC proliferation and migration, the activation of ERK1/2 and AKT was analyzed by assessing ERK1/2 and AKT phosphorylation. We found that the phosphorylation of ERK1/2 and AKT was rapidly increased by the treatment of PDGF-BB for 15 min (Fig. 6, A and B). It is noteworthy that the phosphorylation level of ERK1/2, but not AKT, was markedly inhibited in the presence of vinpocetine in a dose-dependent manner. This suggests that vinpocetine specifically inhibits PDGF-BB-induced ERK1/2 activation.

Vinpocetine Suppresses ROS Production in SMCs. ROS play key roles in cell proliferation, migration, and ECM synthesis in vascular cells (Taniyama and Griendling, 2003; Lyle and Griendling, 2006). It has been previously shown that PDGF induces production of ROS such as H_2O_2, which stimulates the phosphorylation of ERK1/2 in SMCs (Sundaresan et al., 1995). To examine whether vinpocetine affects PDGF-BB-induced ROS production, we assessed ROS by using $DCFH_2$-DA as a probe. We found that PDGF-BB induced a profound increase of ROS as measured by fluorescent microscopy (Fig. 6C) and flow cytometry (Fig. 6D). However, vinpocetine significantly reduced PDGF-BB-induced ROS production (Fig. 6D). To further determine whether ROS is a primary target of vinpocetine in PDGF-stimulated SMC growth, we treated SMCs with submaximal doses of antioxidant *N*-acetyl-L-cysteine (NAC), vinpocetine, or both followed by PDGF stimulation. It is noteworthy that we found that in the presence of NAC vinpocetine barely has an additional effect on attenuation of SMC growth (Fig. 6E). Consistent with the effect of vinpocetine on ERK1/2 and AKT, NAC attenuated ERK1/2 but not AKT phosphorylation stimulated by PDGF-BB (Fig. 6F). In addition, NAC and vinpocetine together have no additive effect on ERK1/2 phosphorylation (Fig. 6F). We obtained similar observations using another antioxidant, tiron (data not shown). These results suggest that the effects of vinpocetine on SMC growth and ERK1/2 activation are at least partially mediated by antagonizing ROS production.

Discussion

In the present study, we demonstrate that systemically applied vinpocetine inhibits injury-induced intimal hyperplasia and vascular thrombosis (Fig. 1; Supplemental Fig. 1S). In addition, we cultured human saphenous vein in an

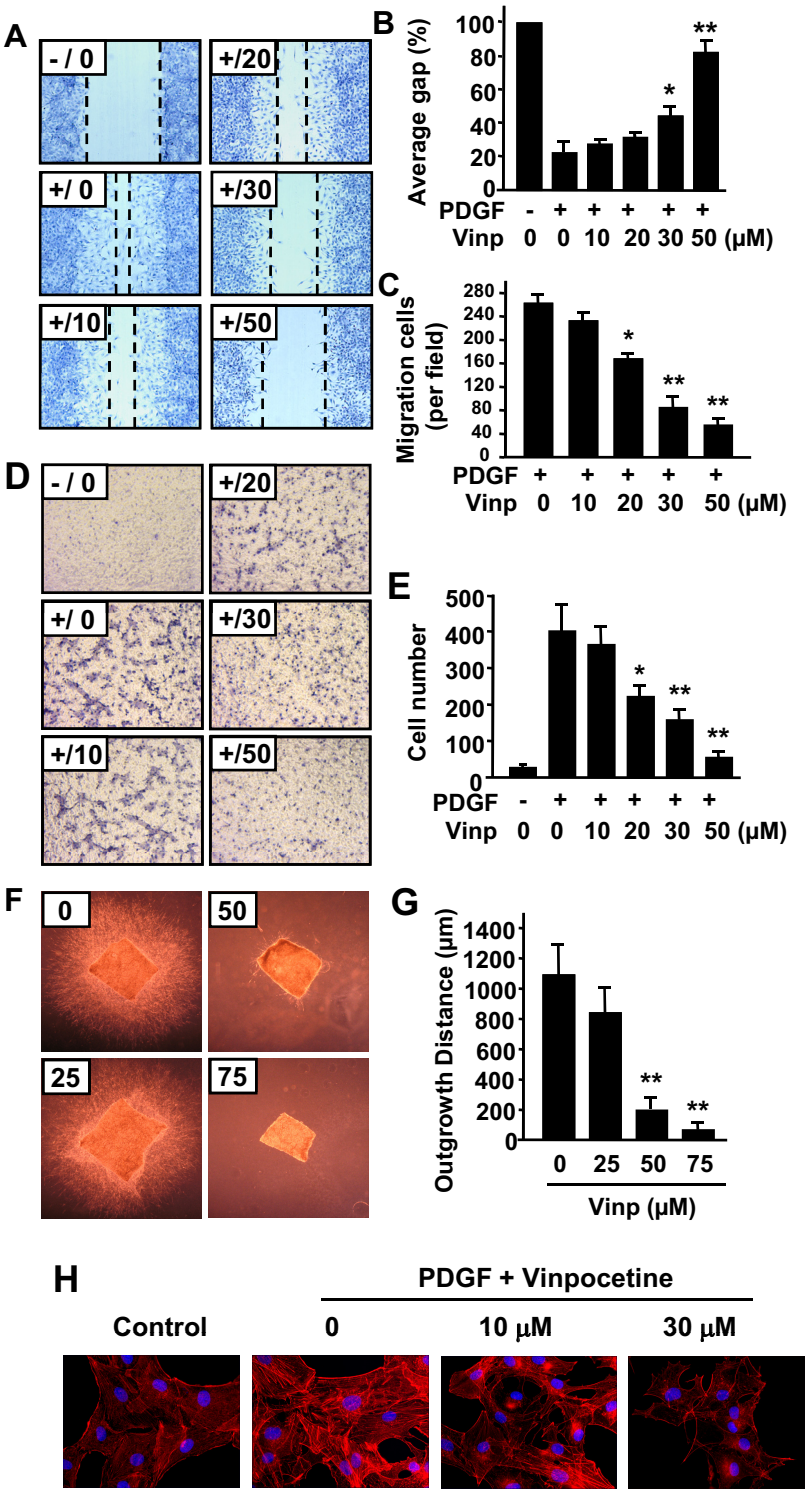

Fig. 4. Effects of vinpocetine on VSMC migration. A to C, scratch wound assay. A, representative images show that vinpocetine dose-dependently inhibited PDGF-induced migration of VSMCs by scratch wound assay. Dotted lines show the edges of cell migration. Confluent VSMCs were starved and scratched with a pipette tip, then treated with vinpocetine at the indicated doses and stimulated with 25 ng/ml of PDGF-BB for 16 h. The cells were fixed with 4% paraformaldehyde and stained with hematoxylin. B and C, quantitative data of the scratch wound assay were analyzed by the percentage of gap area (B) or migrating cell numbers (C). D and E, Boyden chamber assay. D, representative images show that vinpocetine dose-dependently inhibited PDGF-induced transmigration of VSMCs by Boyden chamber assay. One hundred microliters of VSMC suspension was placed in the upper microchemotaxis chamber, and 600 μl of DMEM containing 25 ng/ml of PDGF-BB was placed in the lower polycarbonate filter chamber. The chamber was incubated at 37°C and 5% CO_2 for 6 h. E, the transmigrated cells on the filter membrane were fixed and stained with hematoxylin and quantified. F and G, ex vivo aortic medial explant migration assay. F, representative images show that vinpocetine dose-dependently inhibited PDGF-induced VSMC outgrowth in 3D collagen I gel. Media explants of mouse aorta were embedded in 3D gel containing collagen type I, and the migration of VSMCs was initiated by addition of PDGF-BB/FGF2. G, migration was quantified by measuring the distance migrated by the leading front of VSMCs from the explanted tissue. Values are means ± S.D. from at least three independent experiments. *, $P < 0.05$; **, $P < 0.01$ versus PDGF with no vinpocetine. H, effects of vinpocetine on actin cytoskeleton polymerization in VSMCs. VSMCs were seeded in six-well plates overnight in DMEM supplemented with 10% FBS, serum-starved for 48 h, and treated with or without vinpocetine for 0.5 h, then stimulated with 20 ng/ml of PDGF-BB for 24 h. F-actin was stained by Alexa Fluor 546 phalloidin (red), and nucleus was stained by DAPI (blue).

ex vivo explant model and further confirmed that vinpocetine reduces human saphenous vein remodeling (Fig. 2). These results revealed the novel and important pharmacological effects of vinpocetine on preventing pathological vascular remodeling. Pathological vascular remodeling is involved in the pathogenesis of various vascular disorders that lead to myocardial infarction, stroke, peripheral vascular diseases, or graft failure in organ transplantation. Given that vinpocetine has proven to be a safe drug in long-term therapy (Balestreri et al., 1987), vinpocetine may represent an attractive therapeutic candidate for treating various vascular diseases.

Many vascular diseases are defined as vascular proliferative disorders caused by abnormal proliferation of vascular cells such as SMCs (Braun-Dullaeus et al., 1998). Therefore, the treatment of these diseases, such as restenosis after percutaneous coronary intervention, has focused on targeting the cell cycle. The central regulatory protein complexes involved in the cell cycle are the cyclins and cyclin-dependent kinases (Braun-Dullaeus et al., 1998). When cells are stim-

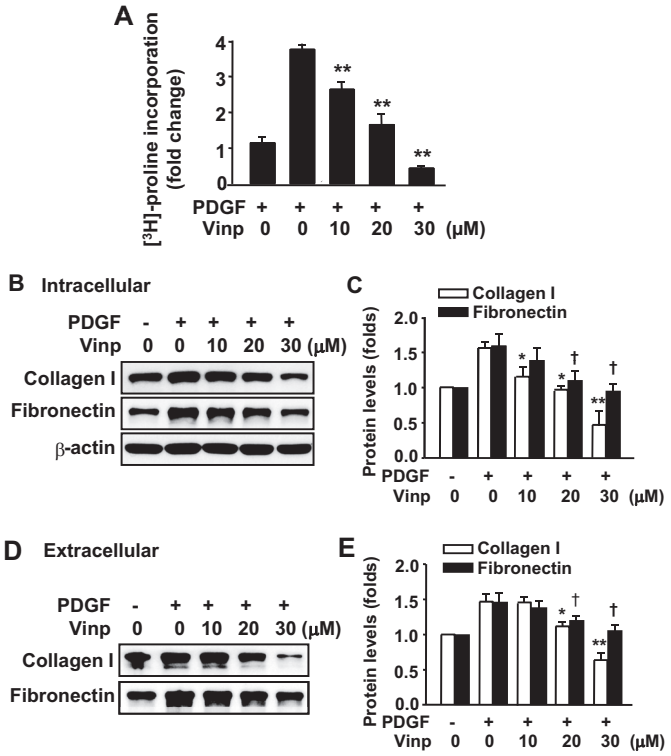

Fig. 5. Effects of vinpocetine on ECM production in VSMCs. A, vinpocetine dose-dependently inhibited PDGF-induced total collagen synthesis measured by [^{3}H]proline incorporation. VSMCs were serum-starved for 48 h, then treated with vinpocetine at the indicated doses and stimulated with 20 ng/ml PDGF-BB for 48 h. Total collagen synthesis was determined by [^{3}H]proline incorporation. B and C, vinpocetine dose-dependently inhibited PDGF-induced expression of collagen I and fibronectin in VSMCs (C) determined by Western blot (B). D and E, vinpocetine inhibited PDGF-induced secretion of collagen I and fibronectin. VSMCs were serum-starved for 48 h, then treated with vinpocetine at the indicated doses and stimulated with 20 ng/ml of PDGF-BB for 48 h (E). The culture media were collected and filtered, then subjected to Western blot (D). *, $P < 0.05$; **, $P < 0.01$ versus PDGF with no vinpocetine (for collagen I). †, $P < 0.05$ versus PDGF with no vinpocetine (for fibronectin).

ulated with growth factors, cell cycle progression occurs. The checkpoints for the G_1/S and G_2/M phases are critical for cell progression. Rapamycin (sirolimus) and paclitaxel (Taxol; Bristol-Myers Squibb Co., Stamford, CT) have been used to coat drug-eluting stents to prevent in-stent restenosis and arrest G_1/S phase transition by up-regulating $p27^{Kip1}$ or $p21^{Cip1}$, therefore inhibiting SMC proliferation (Moses et al., 2003; Stone et al., 2004). In this study, we found that vinpocetine markedly up-regulated levels of $p27^{Kip1}$ and down-regulated cyclin D1, consequently blocking the G_1/S progression of the cell cycle in cultured SMCs in vitro. More importantly, we found that vinpocetine significantly reduced the number of proliferating cells in the neointima of injured mouse carotid arteries (Fig. 1) and in human saphenous veins undergoing remodeling (Fig. 2). These findings highlight the antimitotic effect of vinpocetine in SMCs and suggest that vinpocetine might represent a systemically safe drug for treating vascular proliferative disorders.

Both ERK1/2 and AKT are the important downstream signaling molecules for PDGF-induced SMC proliferation and migration (Muller, 1997). In the present study, we show that vinpocetine and antioxidants (NAC or tiron) inhibit PDGF-BB-induced ERK1/2 but not AKT phosphorylation (Fig. 6). The differential actions on ERK1/2 and AKT have been reported previously. For example, corynoxeine from the Chinese herb (Kim et al., 2008) or knockdown of nonreceptor tyrosine kinase Abl (Jia et al., 2012) attenuated PDGF-induced ERK1/2 phosphorylation but not AKT. In contrast, nitric oxide (Sandirasegarane et al., 2000) as well as bioflavonoids such as tangeretin (Seo et al., 2011), quercetin (Ishizawa et al., 2009), or cudraflavanone (Han et al., 2007), inhibit PGDF-BB-induced SMC proliferation and migration by blocking AKT but not ERK1/2 activation. Together, these observations suggest that ERK1/2 and AKT differentially regulate SMC growth/migration through distinct signaling pathways. The function of ERK1/2 in SMC proliferation/migration and neointima formation is very well established (Izumi et al., 2001; Zhan et al., 2003; Gerthoffer, 2007). ROS such as H_2O_2 have been shown to be key mediators in PDGF-stimulated ERK1/2 activation in SMCs (Sundaresan et al., 1995). Antioxidants attenuate PDGF signaling, SMC growth, and neointima formation (Kappert et al., 2006). We demonstrate, in the present study, that vinpocetine markedly inhibits intracellular ROS generation induced by PDGF (Fig. 6). More importantly, vinpocetine and antioxidants elicit similar effects on ERK1/2 activation and SMC growth, and there is no additive effect when combining vinpocetine and antioxidants (Figs. 3 and 6). These suggest that vinpocetine inhibits ERK1/2 activation and antagonizes SMC proliferation/migration at least partially through suppressing ROS production. Vinpocetine also elicits an antioxidant effect in neurons (Santos et al., 2000). The molecular mechanism by which PDE1C inhibits ROS production needs to be further characterized.

PDE1 was the first molecular target identified for vinpocetine (Bönöczk et al., 2000), and PDE1 also plays a critical role in SMC growth (Nagel et al., 2006). However, the mechanisms underlying SMC growth suppression by vinpocetine or PDE1 inhibition seem to be different. For example, inhibiting nuclear PDE1A function attenuates SMC growth through up-regulating PP2A B56γ expression and promoting β-catenin protein degradation (Jeon et al., 2010a). The PDE1-selective inhibitor IC86340 (Nagel et al., 2006) does not directly affect PDGF-BB-induced ERK1/2 phosphorylation (unpublished observations). In addition, vinpocetine is an IKK inhibitor (Jeon et al., 2010b). IKK/nuclear factor-κB signaling is implicated in smooth muscle cell proliferation and migration (Zahradka et al., 2002; Chung et al., 2009) and injury-induced neointima formation (Zuckerbraun et al., 2003; Grassia et al., 2010). Moreover, vinpocetine is a potent voltage-gated sodium channel blocker (Bönöczk et al., 2000). The voltage-gated sodium channel has been found in several types of SMCs, and these channels seem to be important for SMC migration but not proliferation (Platoshyn et al., 2005; Meguro et al., 2009). Besides SMCs, the anti-inflammatory effects of vinpocetine on vascular cells and macrophages (Jeon et al., 2010b) may contribute to the inhibitory effects of vinpocetine in neointima formation. Vinpocetine has previously been reported to have an antithrombotic effect (Kiss and Kárpáti, 1996) and an endothelial cell-protective effect (Vaizova et al., 2006). Collectively, the protective effects of vinpocetine on pathological remodeling could be attributed to different mechanisms involving multiple cellular targets and cell types, which make vinpocetine as an attractive therapeutic agent in combating vascular disorders.

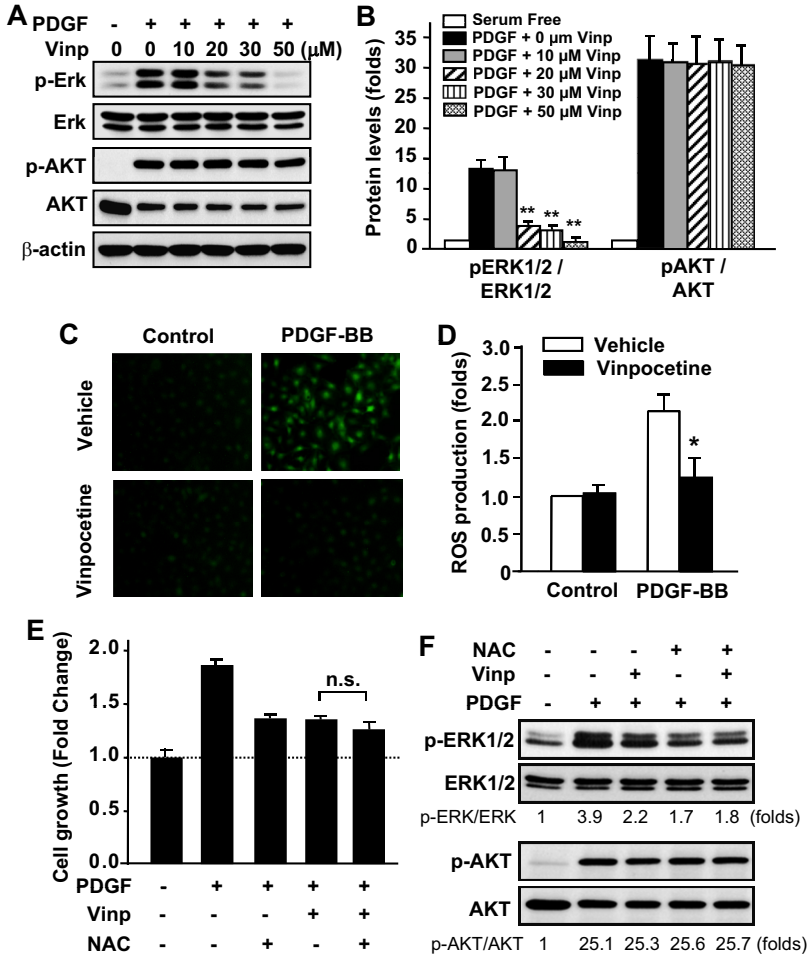

Fig. 6. Effects of vinpocetine on PDGF-induced ERK1/2 and AKT phosphorylation and ROS production in VSMCs. A and B, VSMCs were serum-starved for 48 h, then treated with vinpocetine at the indicated doses and stimulated with 20 ng/ml of PDGF-BB for 15 min. ERK1/2 (A) and AKT (B) phosphorylation and total ERK1/2 and AKT levels were measured by Western blotting with phospho-specific antibodies and total antibodies, respectively. **, $P < 0.01$ versus PDGF with no vinpocetine. C and D, serum-starved VSMCs were labeled with 10 μM $DCFH_2$-DA, then treated with vinpocetine and stimulated with 20 ng/ml of PDGF-BB for 1 h. C, the photographs were taken by using an Olympus (BX-51) fluorescent microscope. D, intracellular ROS was quantified by flow cytometry. *, $P < 0.05$ versus PDGF with vehicle. E, serum-starved VSMCs were pretreated with 30 μM vinpocetine, 5 mM NAC, or both, followed by PDGF-BB (50 ng/ml) stimulation for 48 h. Cell growth was measured by SRB assay. n.s., not significant. F, serum-starved VSMCs were pretreated with 30 μM vinpocetine, 5 mM NAC, or both, followed by PDGF-BB (50 ng/ml) stimulation for 15 min. ERK1/2 and AKT phosphorylation and total ERK1/2 and AKT levels were measured by Western blotting. The blots were analyzed by densitometry. Fold changes normalized to the left lane are shown below the blots ($n = 2–3$).

Acknowledgments

We thank Dr. Jun-ichi Abe (University of Rochester, Rochester, NY) for assistance with real-time PCR.

Authorship Contributions

Participated in research design: Cai, Li, and Yan.

Conducted experiments: Cai and Guo.

Contributed new reagents or analytic tools: P. A. Knight.

Performed data analysis: Cai, Li, and Yan.

Wrote or contributed to the writing of the manuscript: Cai, W. E. Knight, Li, P. A. Knight, and Yan.

References

Adiguzel E, Ahmad PJ, Franco C, and Bendeck MP (2009) Collagens in the progression and complications of atherosclerosis. *Vasc Med* **14:**73–89.

Andrae J, Gallini R, and Betsholtz C (2008) Role of platelet-derived growth factors in physiology and medicine. *Genes Dev* **22:**1276–1312.

Bagoly E, Fehér G, and Szapáry L (2007) [The role of vinpocetine in the treatment of cerebrovascular diseases based in human studies]. *Orv Hetil* **148:**1353–1358.

Balestreri R, Fontana L, and Astengo F (1987) A double-blind placebo controlled evaluation of the safety and efficacy of vinpocetine in the treatment of patients with chronic vascular senile cerebral dysfunction. *J Am Geriatr Soc* **35:**425–430.

Bhardwaj S, Roy H, and Ylä-Herttuala S (2008) Gene therapy to prevent occlusion of venous bypass grafts. *Expert Rev Cardiovasc Ther* **6:**641–652.

Bönöczk P, Gulyás B, Adam-Vizi V, Nemes A, Kárpáti E, Kiss B, Kapás M, Szántay C, Koncz I, Zelles T, et al. (2000) Role of sodium channel inhibition in neuroprotection: effect of vinpocetine. *Brain Res Bull* **53:**245–254.

Braun-Dullaeus RC, Mann MJ, and Dzau VJ (1998) Cell cycle progression: new therapeutic target for vascular proliferative disease. *Circulation* **98:**82–89.

Cai Y, Miller CL, Nagel DJ, Jeon KI, Lim S, Gao P, Knight PA, and Yan C (2011) Cyclic nucleotide phosphodiesterase 1 regulates lysosome-dependent type I collagen protein degradation in vascular smooth muscle cells. *Arterioscler Thromb Vasc Biol* **31:**616–623.

Cai YJ, Lu JJ, Zhu H, Xie H, Huang M, Lin LP, Zhang XW, and Ding J (2008) Salvicine triggers DNA double-strand breaks and apoptosis by GSH-depletion-driven H_2O_2 generation and topoisomerase II inhibition. *Free Radic Biol Med* **45:**627–635.

Callera GE, Touyz RM, Tostes RC, Yogi A, He Y, Malkinson S, and Schiffrin EL (2005) Aldosterone activates vascular p38MAP kinase and NADPH oxidase via c-Src. *Hypertension* **45:**773–779.

Chung CH, Lin KT, Chang CH, Peng HC, and Huang TF (2009) The integrin α2β1 agonist, aggretin, promotes proliferation and migration of VSMC through NF-κB translocation and PDGF production. *Br J Pharmacol* **156:**846–856.

Doran AC, Meller N, and McNamara CA (2008) Role of smooth muscle cells in the initiation and early progression of atherosclerosis. *Arterioscler Thromb Vasc Biol* **28:**812–819.

Filippov S, Koenig GC, Chun TH, Hotary KB, Ota I, Bugge TH, Roberts JD, Fay WP, Birkedal-Hansen H, Holmbeck K, et al. (2005) MT1-matrix metalloproteinase directs arterial wall invasion and neointima formation by vascular smooth muscle cells. *J Exp Med* **202:**663–671.

Gerthoffer WT (2007) Mechanisms of vascular smooth muscle cell migration. *Circ Res* **100:**607–621.

Goncharova EA, Goncharov DA, and Krymskaya VP (2006) Assays for in vitro monitoring of human airway smooth muscle (ASM) and human pulmonary arterial vascular smooth muscle (VSM) cell migration. *Nat Protoc* **1:**2933–2939.

Grassia G, Maddaluno M, Musilli C, De Stefano D, Carnuccio R, Di Lauro MV, Parratt CA, Kennedy S, Di Meglio P, Ianaro A, et al. (2010) The IκB kinase inhibitor nuclear factor-κB essential modulator-binding domain peptide for inhibition of injury-induced neointimal formation. *Arterioscler Thromb Vasc Biol* **30:**2458–2466.

Han HJ, Kim TJ, Jin YR, Hong SS, Hwang JH, Hwang BY, Lee KH, Park TK, and Yun YP (2007) Cudraflavanone A, a flavonoid isolated from the root bark of *Cudrania tricuspidata*, inhibits vascular smooth muscle cell growth via an Akt-dependent pathway. *Planta Med* **73:**1163–1168.

Institute of Laboratory Animal Resources (1996) *Guide for the Care and Use of Laboratory Animals* 7th ed. Institute of Laboratory Animal Resources, Commission on Life Sciences, National Research Council, Washington, DC.

Ishizawa K, Izawa-Ishizawa Y, Ohnishi S, Motobayashi Y, Kawazoe K, Hamano S, Tsuchiya K, Tomita S, Minakuchi K, and Tamaki T (2009) Quercetin glucuronide inhibits cell migration and proliferation by platelet-derived growth factor in vascular smooth muscle cells. *J Pharmacol Sci* **109:**257–264.

Izumi Y, Kim S, Namba M, Yasumoto H, Miyazaki H, Hoshiga M, Kaneda Y, Morishita R, Zhan Y, and Iwao H (2001) Gene transfer of dominant-negative mutants of extracellular signal-regulated kinase and c-Jun NH_2-terminal kinase

prevents neointimal formation in balloon-injured rat artery. *Circ Res* **88:**1120–1126.
Jeon KI, Jono H, Miller CL, Cai Y, Lim S, Liu X, Gao P, Abe J, Li JD, and Yan C (2010a) Ca^{2+}/calmodulin-stimulated PDE1 regulates the β-catenin/TCF signaling through PP2A B56 γ subunit in proliferating vascular smooth muscle cells. *FEBS J* **277:**5026–5039.
Jeon KI, Xu X, Aizawa T, Lim JH, Jono H, Kwon DS, Abe J, Berk BC, Li JD, and Yan C (2010b) Vinpocetine inhibits NF-κB-dependent inflammation via an IKK-dependent but PDE-independent mechanism. *Proc Natl Acad Sci U S A* **107:**9795–9800.
Jia L, Wang R, and Tang DD (2012) Abl regulates smooth muscle cell proliferation by modulating actin dynamics and ERK1/2 activation. *Am J Physiol Cell Physiol* **302:**C1026–C1034.
Kappert K, Sparwel J, Sandin A, Seiler A, Siebolts U, Leppänen O, Rosenkranz S, and Ostman A (2006) Antioxidants relieve phosphatase inhibition and reduce PDGF signaling in cultured VSMCs and in restenosis. *Arterioscler Thromb Vasc Biol* **26:**2644–2651.
Kearney M, Pieczek A, Haley L, Losordo DW, Andres V, Schainfeld R, Rosenfield K, and Isner JM (1997) Histopathology of in-stent restenosis in patients with peripheral artery disease. *Circulation* **95:**1998–2002.
Kim D, Rybalkin SD, Pi X, Wang Y, Zhang C, Munzel T, Beavo JA, Berk BC, and Yan C (2001) Upregulation of phosphodiesterase 1A1 expression is associated with the development of nitrate tolerance. *Circulation* **104:**2338–2343.
Kim TJ, Lee JH, Lee JJ, Yu JY, Hwang BY, Ye SK, Shujuan L, Gao L, Pyo MY, and Yun YP (2008) Corynoxeine isolated from the hook of *Uncaria rhynchophylla* inhibits rat aortic vascular smooth muscle cell proliferation through the blocking of extracellular signal regulated kinase 1/2 phosphorylation. *Biol Pharm Bull* **31:**2073–2078.
Kiss B and Kárpáti E (1996) [Mechanism of action of vinpocetine]. *Acta Pharm Hung* **66:**213–224.
Kumar A and Lindner V (1997) Remodeling with neointima formation in the mouse carotid artery after cessation of blood flow. *Arterioscler Thromb Vasc Biol* **17:**2238–2244.
Liang CC, Park AY, and Guan JL (2007) In vitro scratch assay: a convenient and inexpensive method for analysis of cell migration in vitro. *Nat Protoc* **2:**329–333.
Lyle AN and Griendling KK (2006) Modulation of vascular smooth muscle signaling by reactive oxygen species. *Physiology (Bethesda)* **21:**269–280.
Meguro K, Iida H, Takano H, Morita T, Sata M, Nagai R, and Nakajima T (2009) Function and role of voltage-gated sodium channel NaV1.7 expressed in aortic smooth muscle cells. *Am J Physiol Heart Circ Physiol* **296:**H211–219.
Mekontso-Dessap A, Kirsch M, Guignambert C, Zadigue P, Adnot S, Loisance D, and Eddahibi S (2006) Vascular-wall remodeling of 3 human bypass vessels: organ culture and smooth muscle cell properties. *J Thorac Cardiovasc Surg* **131:**651–658.
Mitchell RN and Libby P (2007) Vascular remodeling in transplant vasculopathy. *Circ Res* **100:**967–978.
Moses JW, Leon MB, Popma JJ, Fitzgerald PJ, Holmes DR, O'Shaughnessy C, Caputo RP, Kereiakes DJ, Williams DO, Teirstein PS, et al. (2003) Sirolimus-eluting stents versus standard stents in patients with stenosis in a native coronary artery. *N Engl J Med* **349:**1315–1323.
Muller DW (1997) The role of proto-oncogenes in coronary restenosis. *Prog Cardiovasc Dis* **40:**117–128.
Nagel DJ, Aizawa T, Jeon KI, Liu W, Mohan A, Wei H, Miano JM, Florio VA, Gao P, Korshunov VA, et al. (2006) Role of nuclear Ca^{2+}/calmodulin-stimulated phosphodiesterase 1A in vascular smooth muscle cell growth and survival. *Circ Res* **98:**777–784.
Owens GK, Kumar MS, and Wamhoff BR (2004) Molecular regulation of vascular smooth muscle cell differentiation in development and disease. *Physiol Rev* **84:**767–801.
Pendyala LK, Yin X, Li J, Chen JP, Chronos N, and Hou D (2009) The first-generation drug-eluting stents and coronary endothelial dysfunction. *JACC Cardiovasc Interv* **2:**1169–1177.
Platoshyn O, Remillard CV, Fantozzi I, Sison T, and Yuan JX (2005) Identification of functional voltage-gated Na^+ channels in cultured human pulmonary artery smooth muscle cells. *Pflugers Arch* **451:**380–387.
Porter KE, Varty K, Jones L, Bell PR, and London NJ (1996) Human saphenous vein organ culture: a useful model of intimal hyperplasia? *Eur J Vasc Endovasc Surg* **11:**48–58.
Raines EW (2004) PDGF and cardiovascular disease. *Cytokine Growth Factor Rev* **15:**237–254.
Ranjzad P, Salem HK, and Kingston PA (2009) Adenovirus-mediated gene transfer of fibromodulin inhibits neointimal hyperplasia in an organ culture model of human saphenous vein graft disease. *Gene Ther* **16:**1154–1162.
Ross R (1993) The pathogenesis of atherosclerosis: a perspective for the 1990s. *Nature* **362:**801–809.
Sandirasegarane L, Charles R, Bourbon N, and Kester M (2000) NO regulates PDGF-induced activation of PKB but not ERK in A7r5 cells: implications for vascular growth arrest. *Am J Physiol Cell Physiol* **279:**C225–C235.
Santos MS, Duarte AI, Moreira PI, and Oliveira CR (2000) Synaptosomal response to oxidative stress: effect of vinpocetine. *Free Radic Res* **32:**57–66.
Sartore S, Chiavegato A, Faggin E, Franch R, Puato M, Ausoni S, and Pauletto P (2001) Contribution of adventitial fibroblasts to neointima formation and vascular remodeling: from innocent bystander to active participant. *Circ Res* **89:**1111–1121.
Sata M, Saiura A, Kunisato A, Tojo A, Okada S, Tokuhisa T, Hirai H, Makuuchi M, Hirata Y, and Nagai R (2002) Hematopoietic stem cells differentiate into vascular cells that participate in the pathogenesis of atherosclerosis. *Nat Med* **8:**403–409.
Schwartz RS and Henry TD (2002) Pathophysiology of coronary artery restenosis. *Rev Cardiovasc Med* **3 (Suppl 5)**:S4–S9.
Seo J, Lee HS, Ryoo S, Seo JH, Min BS, and Lee JH (2011) Tangeretin, a citrus flavonoid, inhibits PGDF-BB-induced proliferation and migration of aortic smooth muscle cells by blocking AKT activation. *Eur J Pharmacol* **673:**56–64.
Stone GW, Ellis SG, Cox DA, Hermiller J, O'Shaughnessy C, Mann JT, Turco M, Caputo R, Bergin P, Greenberg J, et al. (2004) A polymer-based, paclitaxel-eluting stent in patients with coronary artery disease. *N Engl J Med* **350:**221–231.
Sundaresan M, Yu ZX, Ferrans VJ, Irani K, and Finkel T (1995) Requirement for generation of H_2O_2 for platelet-derived growth factor signal transduction. *Science* **270:**296–299.
Szobor A and Klein M (1976) Ethyl apovincaminate therapy in neurovascular diseases. *Arzneimittelforschung* **26:**1984–1989.
Tamaki N and Matsumoto S (1985) [Agents to improve cerebrovascular circulation and cerebral metabolism–vinpocetine]. *Nippon Rinsho* **43:**376–378.
Taniyama Y and Griendling KK (2003) Reactive oxygen species in the vasculature: molecular and cellular mechanisms. *Hypertension* **42:**1075–1081.
Torsney E and Xu Q (2011) Resident vascular progenitor cells. *J Mol Cell Cardiol* **50:**304–311.
Vaizova OE, Vengerovskii AI, and Alifirova VM (2006) [An effect of vinpocetine (cavinton) on endothelium function in patients with chronic cerebral ischemia]. *Zh Nevrol Psikhiatr Im S S Korsakova* **Suppl 16:**46–50.
Vichai V and Kirtikara K (2006) Sulforhodamine B colorimetric assay for cytotoxicity screening. *Nat Protoc* **1:**1112–1116.
Zahradka P, Werner JP, Buhay S, Litchie B, Helwer G, and Thomas S (2002) NF-κB activation is essential for angiotensin II-dependent proliferation and migration of vascular smooth muscle cells. *J Mol Cell Cardiol* **34:**1609–1621.
Zhan Y, Kim S, Izumi Y, Izumiya Y, Nakao T, Miyazaki H, and Iwao H (2003) Role of JNK, p38, and ERK in platelet-derived growth factor-induced vascular proliferation, migration, and gene expression. *Arterioscler Thromb Vasc Biol* **23:**795–801.
Zuckerbraun BS, McCloskey CA, Mahidhara RS, Kim PK, Taylor BS, and Tzeng E (2003) Overexpression of mutated IκBα inhibits vascular smooth muscle cell proliferation and intimal hyperplasia formation. *J Vasc Surg* **38:**812–819.

Address correspondence to: Dr. Chen Yan, Aab Cardiovascular Research Institute, University of Rochester School of Medicine and Dentistry, 601 Elmwood Ave, Box CVRI, Rochester, NY 14642. E-mail: Chen_Yan@urmc.rochester.edu